

Algorithms for Feature Extraction from Synthetic Aperture Radar Data

Sowmyashree M.V.¹

sowmyashree@ces.iisc.ernet.in

¹Energy & Wetlands Research Group, Centre for Ecological Sciences [CES], IISc²Centre for Sustainable Technologies (astra)³Centre for infrastructure, Sustainable Transportation and Urban Planning [CiSTUP]

Indian Institute of Science, Bangalore, Karnataka, 560 012, India

Web: <http://ces.iisc.ernet.in/energy>, <http://ces.iisc.ernet.in/foss>Ramachandra T.V.^{1,2,3}

cestvr@ces.iisc.ernet.in

Abstract— Earth's surface consists of land features such as vegetation, soil, water, etc. Modeling of the earth's surface requires identification and understanding of the dynamics of land features. Analysis of land feature dynamics would reveal the changes that occur due to human induced activities or natural phenomenon. This plays a major role in providing up-to-date information of the natural resources. Data acquired remotely through space-borne sensors at regular intervals in visible and microwave bands aid in spatial mapping of the land features. Data acquired in visible and IR (Infrared) bands have been used for land use and land cover analysis. However, these data fails when there are cloud cover due to non-selective scattering. In this context, RADAR remote sensing would be useful as it provide information during all seasons due to long penetration properties. In present study, RADARSAT-2 single polarized HH (i.e., Horizontal to Horizontal with C- band) has been used to derive land features with spatial extent. Radar data interpretation and analysis is considered challenging and have both advantages and disadvantages in land use feature extraction. This study assess the performance of classification algorithms (Gaussian Maximum likelihood classifier (GMLC), Neural network classifier, Decision tree classifier (DTC), Contextual classification using sequential maximum a posteriori (SMAP) estimation for feature extraction using multi-temporal single polarized RADARSAT data, texture extracted data and fused data (optical sensor -LANDSAT ETM+ with SAR data). Accuracy assessments suggest that fused data perform better with all algorithms.

Keywords— Land features; remote sensing SAR- Synthetic Aperture RADAR; feature extraction; classification algorithms; accuracy assessment

I. INTRODUCTION

Land features are the physical characteristics of the Earth's surface. Changes in the physical composition of the Earth happens either due to natural or human induced activities [1]. Land cover [LC] provides the extent of vegetation and non-vegetation referring to the physical cover of the Earth. Land use [LU] provides details of human altered environment which include the extent of land under various uses such as agriculture, plantations, forests, etc [2]. Data acquired through remote sensors at regular intervals enable to derive information of LULC and landscape dynamics. RADAR (Radio Detection and Ranging), an active sensor provides data

under all weather conditions. Radar surface feature interaction and scattering, and the characteristics of this scattered energy or backscattered energy are dependent upon the geometric and electrical factors of the ground features [3].

Assessment of temporal dynamics of these features provides vital inputs for regional planning and sustainable management of natural resources. Applications in agriculture, horticulture, forestry etc. require continuous data during the entire phenology cycle to address the problem of pests, moisture stress, etc. Data acquired through space-borne sensors at regular intervals have been useful to derive the information of Earth's features in cost and time effective way. However, passive remote sensing fails to provide the data in the presence of clouds and higher concentrations of aerosols in the atmosphere. Active remote sensors have overcome this drawback due to its ability to penetrate through clouds to sense Earth features. The terrain features in passive remote sensing (data acquired in visible and IR bands, optical data) depends on the spectral characteristics. Compared to this, active remote sensors (SAR) depend on the amplitude and phase of the returned signal [4]. However, there are challenges in SAR data with speckle noise due to coherent nature of waves scattered back to the sensor from the terrain elements. The interpretation of multi-temporal SAR, texture images requires thorough understanding of backscattering associated with different earth's features. Fusion of optical and SAR data would further improve the interpretation of land features. The effectiveness of fused data for feature extraction is compared with the SAR filtered and texture information. Numerous land feature extraction techniques are being used for classifying the RADAR data. The current work evaluates the performance of most commonly used algorithms for extracting land feature from RADARSAT- HH C-band data.

II. STUDY AREA

Dandeli wild life sanctuary located at 15.267°N 74.617°E at the bank of Kali River in Uttara Kannada district of Karnataka State in India. It is a part of Haliyal and Yellapur Forest Division, Western Ghats of Karnataka. Fig. 1 shows the part of Dandeli forest of Uttara Karnataka district.

We thank NRDMS division, The Ministry of Science and Technology, Government of India and Indian Institute of Science, Bangalore for the financial assistance and infrastructure support. We are grateful to Space Application Centre (SAC), Ahmedabad and Karnataka State Remote sensing Application centre, Bangalore for providing RADAR data for analysis and Global Land Cover Facility, USA for providing the Landsat imagery. We thank Uttam Kumar IIT, Bangalore for suggestions during the discussion.

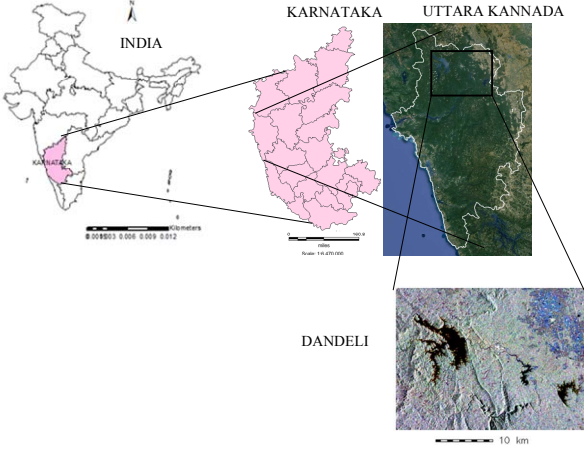


Fig. 1. Dandeli Forest of Uttara Kannada district

III. DATA ACQUISITION

Table I provide the details of RADARSAT-2 and LANDSAT data used in this study. The RADARSAT-2 HH and LANDSAT ETM+ SLC-OFF data have been used in the current analysis. RADARSAT- 2 Horizontal- Horizontal polarization data of 25 m resolution and the incidence angle of the image ranges from 31 to 46° was obtained from Space Applications Centre (SAC, Ahmedabad) through Karnataka State Remote Sensing applications Centre (KSRSAC, Bangalore). Landsat satellite image were downloaded from public domains at GLCF-Global Land Cover Facility (<http://www.glcg.umd.edu/index.shtml> and <http://www.landcover.org/>), USGS Earth Explorer, United States Geological Survey (<http://edcns17.cr.usgs.gov/NewEarthExplorer/>) and Glovis (<http://www.glovis.usgs.gov/>) websites.

TABLE I. RADARSAT AND LANDSAT SATELLITE DATA USED FOR THE ANALYSIS

Sensors	Resolution	Acquisition data
RADARSAT-2 C-band HH	25 m	20 th July 2011, 13 th August 2011,
LANDSAT-ETM+ (SLC OFF)	30 m	24 th November 2011

IV. METHOD

Feature extraction through different classification algorithms were implemented on RADARSAT and LANDSAT ETM+ data. The analyses include preprocessing, geo-rectification, speckle suppression, generation of backscatter co-efficient image and feature extraction (using four classification algorithms i.e., Gaussian Maximum likelihood classification, Decision tree classifier, Neural network and Sequential maximum a posteriori algorithm). Fig. 2 depicts the procedure adopted in the study.

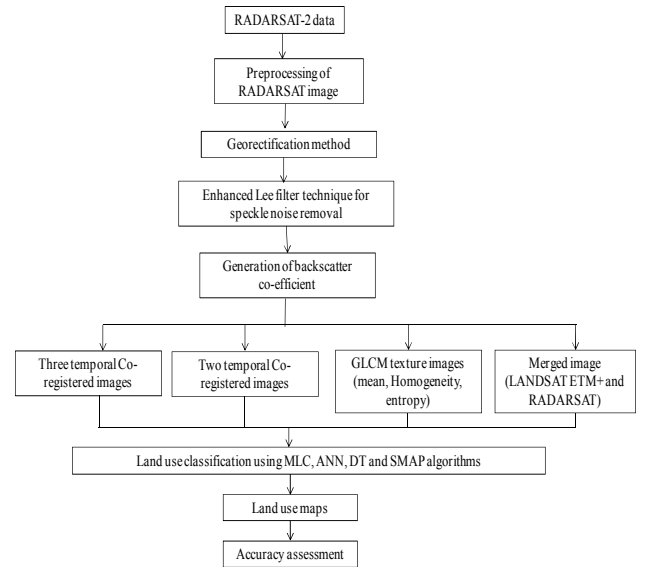


Fig. 2. Procedure adopted in the study

A. Preprocessing of the RADARSAT

Preprocessing of the RADARSAT data includes georeferencing using ground control points and projected to Latitude and longitude WGS84 co-ordinate system, speckle suppression technique was applied on the data Enhance Lee (5 x 5). Finally, the backscatter co-efficient i.e., sigma naught (σ_0) was calculated as in (1),

$$\sigma_0 = [10.0 * \log_{10} (\text{Pixel value})^2 - A_0] * \sin \theta \quad (1)$$

Where, A_0 is the scaling factor and θ is the local incidence angle.

B. Land cover

Land cover is the first level of feature extraction and classification method that helps in understanding land cover types of the region broadly in terms of vegetation and non-vegetation. The vegetation indices indicate the extent of the vegetation and soil in the region. In this study, the Normalized Difference Vegetation Index (NDVI) was used to calculate the land cover types. NDVI is calculated using (2),

$$NDVI = \frac{NIR - RED}{NIR + RED} \quad (2)$$

NDVI values ranges from -1 to 1. The negative value indicates the non-vegetation and presence of built-up, water, sand etc. The increasing value from 0 indicates the presence of vegetation.

C. Land use feature extraction

The extraction of land features such as Built-up, vegetation, water bodies and others was done on four scenarios:

1) *Scenario 1:* Feature extraction technique for three temporal RADARSAT-2 images. In this scenario, three RADARSAT images were co-registered and then used for

feature extraction using four different classification algorithms.

2) *Scenario 2*: Feature extraction technique for two temporal RADARSAT-2 images. In this scenario, two RADARSAT images were co-registered and used for feature extraction using four classification algorithms.

3) *Scenario 3*: Feature extraction using Grey Level Co-occurrence Matrix for texture analysis [5]. Grey level Co-occurrence matrix indicates how often the different combinations of grey levels occur in an image. GLCM parameters provide the variation of different pixel intensities in an image [6]. There are six GLCM texture such as contrast, dissimilarity, mean, entropy, homogeneity and variance. In this study, three texture measures i.e., mean, entropy and homogeneity were considered. Entropy and homogeneity have opposite characteristics and mean gives the mean backscatter co-efficient. Entropy gives the randomness of the intensity values in an image while homogeneity measures the uniformity of an image. The texture measures entropy and homogeneity along with mean backscatter provides complementary information calculated by (2) (3) and (4),

$$Mean = \sum_i \frac{x_i}{n} \quad (2)$$

$$Entropy = \sum_i \sum_j P(i,j) \log P(i,j) \quad (3)$$

$$Homogeneity = \sum_i \sum_j \frac{P(i,j)}{1+|i-j|} \quad (4)$$

'n' is the number of grey values and P (i,j) is the (i,j)th entry of the normalized GLCM matrix.

4) *Scenario 4*: Feature extraction using fused RADARSAT and LANDSAT image. Image fusion is the merging of images and proposed by many researches [7] [8], Image fusion is the combination of High resolution sensor PAN image and Low resolution sensor multispectral image and to produce resultant image with the highest spatial information and good spectral quality. In this study, the image fusion technique using Brovey transformation (as per [9]) was performed on scan line corrected LANDSAT ETM+ (2, 3, 4) bands and RADARSAT -2 image. Brovey transformation is calculated as in (5),

$$DN_{Fused} = \left(\frac{DN_{B1}}{DN_{B1} + DN_{B2} + DN_{B3}} \right) * RADAR_backscatter \quad (5)$$

Where DN_{B1} , DN_{B2} , DN_{B3} are bands of LANDSAT ETM+ and RADAR backscatter is backscattered co-efficient image.

D. Classification Algorithms

The image classification procedures are used to categorize all pixels into land use classes.

1) *Gaussian Maximum likelihood classification*: The maximum likelihood classifier quantitatively evaluates both the variance and covariance of the category spectral response patterns when classifying an unknown pixel. The probability density functions are used to classify an unidentified pixel and

probability of the pixel value belonging to each category is computed. After evaluating the probability in each category, the pixel would be assigned to the most likely class. The disadvantage of GLCM is large number of computation is required to classify the pixel and with less number of training sets, the classification accuracy may decrease [10].

2) *Neural Network*: The difficulties in the conventional digital classification can be overcome by using neural network classification. Unlike GMLC, the neural classifier makes no assumption of probability distribution function of each class. This allows neural networks to be used with a much wider range of types of input data than could be used in a traditional maximum-likelihood algorithm. A Neural Network consists of a set of three or more layers, each made up of multiple nodes. The nodes are also known as "neurons". The three layers include input layer, hidden layer and output layer. The input layer represents the variables used as input to the network and the output layer represents the range of possible outcome categories to be produced by the network. If the network is used for image classification then the output layers consists of nodes with different land use types. In between the input and output layers are one or more hidden layers. The hidden layers consist of many nodes connected to the preceding layers and to the following layers. The linkage between the layers represents the weights, which shows the flow of information. Fig. 3 shows the neural network that is used to classify the images in this study.

ANN classification process basically has three major phases. In the training phase, in which input image with known features (Built-up, vegetation, water bodies and others) are considered as training sites. The backscatter co-efficient information (e.g., Multi-temporal SAR bands or merged optical and SAR images) for each training site is then collected and passed to the input layer of the neural network. In the learning phase, learning is usually accomplished by adjusting the weights using a back-propagation neural network.

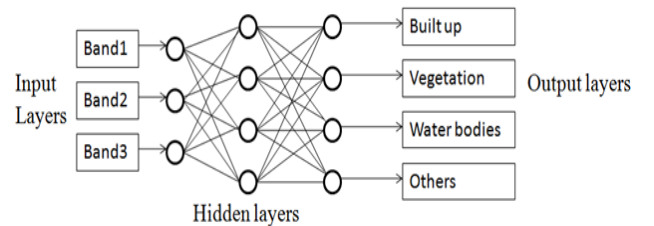


Fig. 3. Neural network architecture used to classify the images

3) *Decision tree Classifier*: Decision tree is inductive learning algorithm that generates classification tree using training data/ samples. It breaks down a problem into two or more sub problem of the same type so that they become simple enough to be solved directly. The solutions of sub-problems are then combined to give a solution to the original problem. It is non-parametric in nature and independent of the properties of the distribution of data, and thus suitable for incorporation of non-spectral data into classification procedure

so that improvement in class separation can be achieved. It is a tree structure where at each branch a specific decision rule is implemented, which involves one or more combinations of the attribute inputs. A new input vector then travels from the root node down through successive nodes until it is classified to particular class. The thresholds used for decisions are chosen based on the minimum entropy. Information gain ratio is used in splitting criteria and the splitting ceases when number of instances to be split is below certain threshold. Information gained by selecting attributes (A_i) or to branch or to partition the data is given by the difference of prior entropy and the entropy of selected branch. The attribute with the highest gain is chosen to split the current tree [11]. The information gain is given as in (6),

$$Gain(D, A_i) = H[D] - H_{A_i}[D] \quad (6)$$

4) *Contextual classification using sequential maximum a posteriori (SMAP) estimation*: SMAP is used to segment multispectral images using a spectral class model known as Gaussian mixture distribution. In current study, the same procedure is used for backscattered multi-temporal RADARSAT images, texture image and fused images (LANDSAT and RADARSAT). The SMAP approach attempts to account for contextual information rather than the pixel-based classification to improve accuracy [12]. SMAP approach (Bouman and Shapiro, 1994), is a Bayesian method which uses both sequential maximum a posteriori estimator in and multi scale random field [12]. It works by segmenting the image at various scales or resolutions and using the coarse scale segmentations to guide the finer scale segmentations. In addition to reducing the number of misclassifications, the SMAP algorithm generally produces segmentations with larger connected regions of a fixed class which may be useful in some applications. The amount of smoothing that is performed in segmentation is dependent of the behavior of the data in the image. If the data suggests that the nearby pixels often change class, then the algorithm will adaptively reduce the amount of smoothing. This ensures that excessively large regions are not formed.

Accuracy assessment was performed through classification error matrix also called as confusion matrix. It is the statistical way of measuring the agreement of classification with the ground data.

V. RESULTS AND DISCUSSION

A. Land cover analysis

The land cover information is generated by NDVI using scan line corrected band 3 (Red band) and band 4 (Infrared band) of LANDSAT ETM+ data. NDVI values (Fig. 4) range from -0.66 to 0.55. Vegetation of the region is about 84.14% and Non vegetation part is about 15.86%. Vegetation covers the Dandeli forest area and plantations. Non vegetation includes soil, water, open spaces.

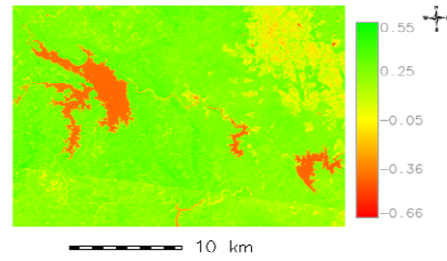


Fig. 4. Land cover using NDVI

B. Land use feature extraction using Classification Algorithms

Scenario 1: Feature extraction technique implemented using the three temporal RADARSAT-HH C-band data. Initially, false color composite (FCC) of three temporal RADARSAT data was generated and training sites were created for each land features i.e., built-up, vegetation, water bodies and others category. Classification was performed using Maximum likelihood algorithm, Neural Network, Decision tree classifier and SMAP. Fig.5 shows the land use maps generated from four algorithms and Table II gives the land feature statistics.

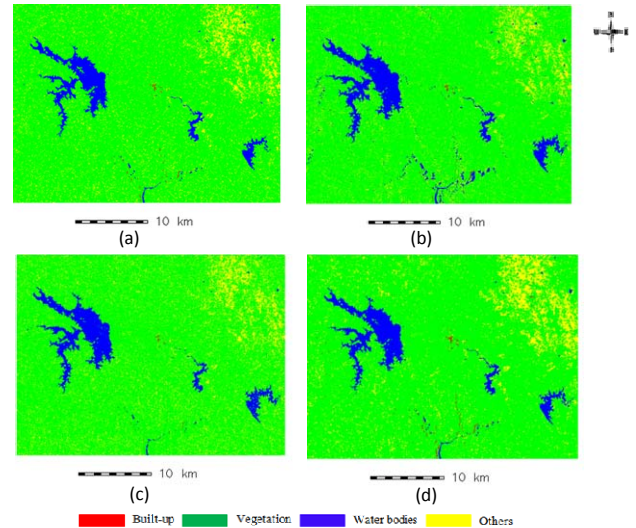


Fig. 5. Land use maps generated using four different algorithms from three temporal Co-registered RADARSAT- HH (a) Maximum likelihood classier (b) Neural Network (c) Decision tree (d) Sequential maximum a posteriori.

TABLE II. LAND FEATURES STATISTICS USING THREE TEMPORAL RADARSAT DATA.

CLASS	GMLC		Neural Network		Decision tree		SMAP	
	Sq.km	%	Sq.km	%	Sq.km	%	Sq.km	%
Built-up	1.6	0.07	1.38	0.06	0.6	0.03	3.65	0.17
Vegetation	1866	86.8	1865	86.73	1812.3	84.4	1863.1	86.6
Water bodies	88.86	4.13	128.4	5.97	107.1	5.0	101.1	4.71
Others	193.3	8.99	155.6	7.24	225.4	10.5	182.4	8.49
Total	2150.4	100	2150	100	2150.4	100	2150.4	100

Scenario 2: Feature extraction technique is implemented for two temporal RADARSAT images. Land use classification procedure performed on the two temporal RADARSAT-HH C-band images. Initially, false color composite (FCC) of two temporal RADARSAT data was generated and training sites were created for each land features i.e., built-up, vegetation, water bodies and others category. Classification process was performed using Maximum likelihood algorithm, Neural Network, Decision tree classifier and SMAP estimation. Fig. 6 shows the land use maps generated from four algorithms for two temporal co-registered images and Table III represents land feature statistics for classified images.

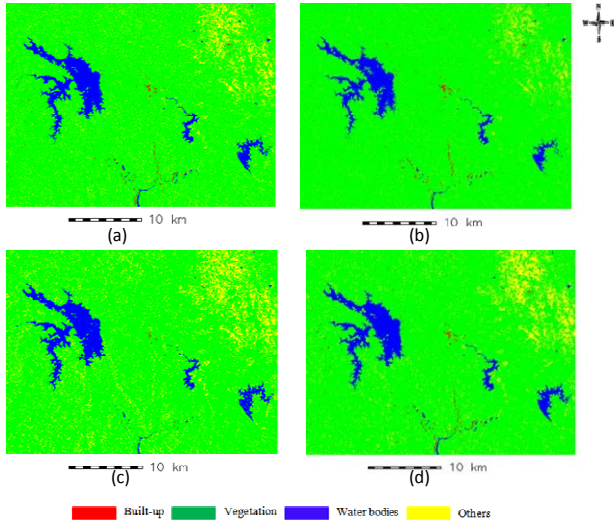


Fig. 6. Land use maps generated using four different algorithms from two temporal Co-registered RADARSAT- HH (a) Maximum likelihood classier (b)Neural Network (c) Decision tree (d) Sequential maximum a posteriori

TABLE III. LAND FEATURE STATISTICS USING TWO TEMPORAL RADARSAT DATA.

CLASS	GMLC		Neural Network		Decision tree		SMAP	
	Sq.km	%	Sq.km	%	Sq.km	%	Sq.km	%
Built-up	4.56	0.21	4.2	0.20	0.60	0.03	4.82	0.2
Vegetation	1869.6	86.9	1895.0	88.78	1836.10	85.7	1898.7	87.3
Water bodies	104.10	4.84	86.9	4.04	107.34	5.01	107.75	5.01
Others	172.12	8.00	164.16	6.98	196.52	9.18	139.06	7.47
Total	2150.4	100	2150.4	100.0	2150.4	100	2150.4	100

Scenario 3: Feature extraction technique from GLCM texture-derived RADARSAT images. GLCM represents the variations in the grey levels with respect to the neighboring pixels. In this study, considered only three texture measures i.e., mean, entropy and homogeneity. Entropy and homogeneity have opposite characteristics and mean gives the mean backscatter co-efficient. Entropy gives the randomness of the intensity values in an image and homogeneity measures the uniformity of an image. Texture images were derived using various window sizes and, 15 x 15 window size proved to be best. Classification process was performed using Maximum likelihood algorithm, Neural Network, Decision tree classifier and SMAP estimation as in Fig. 7 and Table IV gives land

feature statistics for classified output of texture extracted images.

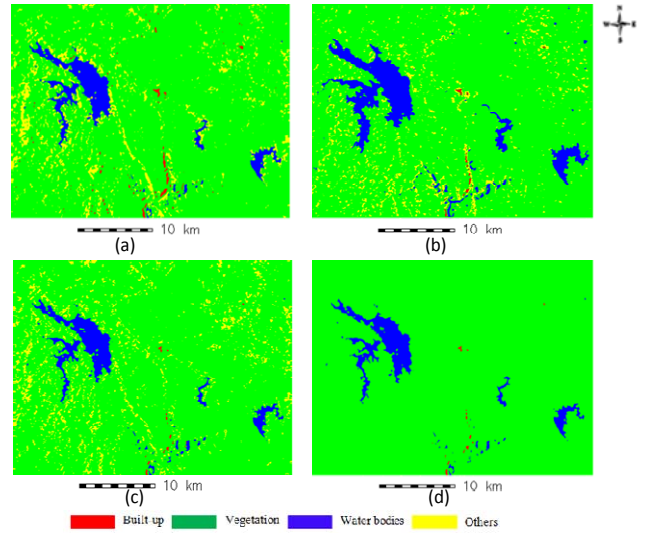


Fig. 7. Land use maps generated using four different from texture extracted RADARSAT – HH images (a) Maximum likelihood classier (b)Neural Network (c) Decision tree (d) Sequential maximum a posteriori

TABLE IV. LAND FEATURE STATISTICS FOR DERIVED FROM TEXTURE EXTRACTED RADARSAT-HH DATA

CLASS	GMLC		Neural Network		Decision tree		SMAP	
	Sq.km	%	Sq.km	%	Sq.km	%	Sq.km	%
Built-up	8.48	0.39	2.49	0.12	1.88	0.09	1.87	0.09
Vegetation	1908.0	88.7	1898.2	88.2	1929.6	89.74	2060	95.80
Water bodies	91.28	4.25	97.01	4.5	87.19	4.05	88.41	4.11
Others	141.8	6.60	152.71	7.1	131.72	6.12	-	-
Total	2150.4	100	2150.4	100	2150.4	100	2150.4	100

Scenario 4: Feature extraction technique from fused RADARSAT-HH and LANDSAT ETM+ SLC-off images.

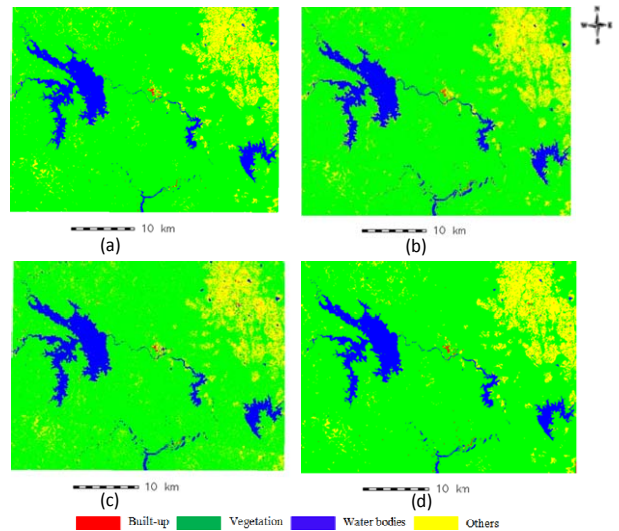


Fig. 8. Land use maps generated using four different algorithms from fused RADARSAT- HH and LANDSAT ETM+ (a)Maximum likelihood classier (b)Neural Network (c)Decision tree classifier (d)Sequential maximum a posteriori.

Landuse classification of RADARSAT and Landsat ETM+ fused images generated by Brovey method using i.fusion.brovey in GRASS GIS. Training sites were created for each land use features i.e., built-up, vegetation, water bodies and others category. Classification process was performed using Maximum likelihood algorithm, Neural Network, Decision tree classifier and SMAP estimation. Fig. 8 shows land use features for four different algorithms from fused RADARSAT- HH and LANDSAT ETM+ and Table V gives the land feature statistics for fused RADARSAT- HH and LANDSAT ETM+ images.

TABLE V. LAND FEATURE STATISTICS FOR FUSED RADARSAT-HH AND LANDSAT ETM+ DATA

CLASS	GMLC		Neural Network		Decision tree		SMAP	
	Sq.km	%	Sq.km	%	Sq.km	%	Sq.km	%
Built-up	1.94	0.0	5.79	0.27	3.90	0.18	2.23	0.10
Vegetation	1800.	84.	1769.8	82.3	1772.2	82.32	1809.7	84.1
Water bodies	151.4	6.6	150.65	7.01	156.23	7.30	136.28	6.34
Others	197.1	9.2	224.10	10.4	218.47	10.20	202.2	9.40
Total	2150.	100	2150.4	100	2150.4	100	2150.4	100

C. Accuracy Assessment

Accuracy assessment was performed on classified images through error matrix. Overall accuracy and kappa statistics were calculated to know best classified output. Table VI shows the overall accuracy and kappa statistics for classified images.

TABLE VI. OVERALL ACCURACY AND KAPPA STATISTICS

Scenario	Overall accuracy				Kappa co-efficient			
	GMLC	NN	DT	SMAP	GMLC	NN	DT	SMAP
1	88.0	88.9	89.6	93.2	0.82	0.82	0.82	0.89
2	88.7	86.4	89.0	91.2	0.82	0.80	0.83	0.85
3	73.0	73.0	79.0	-	0.56	0.56	0.65	-
4	94.3	92.2	93.6	94.2	0.90	0.88	0.89	0.90

For each land use classes, producer's accuracy (PA) and user's accuracy (UA) have been calculated. The PA for built-up class ranged from 60.3% (GLCM) to 81.3% (DT) for three temporal images, and UA ranged from 57.2 (GLCM) to 97.5 (SMAP). PA ranged from 42.6% (GLCM) to 83.5% (DT) for two temporal images, texture images gave lower accuracies with maximum PA of 40% for DT and UA of 60% for SMAP. For fused images, PA ranged from 63.0% (DT) to 99.2% (GLCM) and UA ranged from 38.8% (DT) to 77.7% (GCLM). Similarly, for vegetation category PA ranged from 85.6% (GLCM) to 94.3 (DT) and UA ranged from 59.2% (NN) to 92.9 (SMAP) for three temporal images, two temporal gave better PA for SMAP of 87.6% and UA 94.3% (NN), texture images gave better result for DT (PA - 71.6% and UA-89.4%) and 90% (NN) of PA and 99.7 (SMAP) of UA for fused images. For water bodies, both Producer's accuracy and user's accuracy ranged from 90's to 100% for all scenarios. The others category showed the maximum PA and UA for DT of 88.8% and SMAP of 80.3% for three temporal images, 88.8% (NN) and 68.2% (SMAP), the texture images gave

lower PA and UA and fused images gave better PA of 99.5% (SMAP) and UA of 72% (SMAP).

VI. CONCLUSION

Classification and accuracy assessment indicate that fused RADARSAT- HH and LANDSAT ETM+ provided best result. A comparison of four classification techniques for three temporal and two temporal co-registered RADARSAT-HH image indicated that contextual classification using SMAP estimation proved best with overall accuracy of 93.2% and kappa statistics of 0.89 (three temporal) and overall accuracy of 91.2% and kappa statistics of 0.85 for two temporal classified image. Three temporal co-registered RADARSAT-HH images gave better result than the two temporal Co-registered RADARSAT images. Texture image classification gave lower classification accuracy when compared to three or two composite radar data.

REFERENCES

- [1] Ramachandra, T. V., and Uttam Kumar., "Geoinformatics for Urbanisation and Urban Sprawl pattern analysis." Chapter 19, 2009, pp. 235-272.
- [2] Suresh Y, Balachandar D, Murthy K R, Muganandam R and Kumaraswamy K., "Land use/ Land cover change detection through using remote sensing and GIS techniques- a case study of St. Thomas mount block, Kancheepuram district, Tamilnadu", in International Journal of Current Research vol.3, 2011, pp. 501-504.
- [3] Craig Dobson, M, Ulaby F. T, and Pierce L, E., "Land-cover Classification and estimation of terrain attribute using Synthetic Aperture Radar", in Remote sensing of Environment, vol. 51, 1995, pp. 199-214.
- [4] Gomez-Chova, L, Fernández-Prieto, D, Calpe, J, Soria E, Vila, J and Camps-Valls, G., "Urban monitoring using multi-temporal SAR and multi-spectral data", in Pattern Recognition Letters, vol.27, no. 4, 2006, pp. 234-243.
- [5] Haralick, R. M, Shanmugam K and Dinstein I, H., "Textures Features for Image Classification", systems, Man, and Cybernetics, IEEE Transactions on 6, pp. 610-621, November 1973.
- [6] Hassan H.H and Goussev, S., "Texture Analysis of High Resolution Aeromagnetic Data to Identify Geological Features in the Horn River Basin", NE British Columbia, 2011.
- [7] Carper W.J, Lillesand, T. M, and Ralph W. K., "The use of intensity-hue-saturation transformation for merging SPOT panchromatic and multispectral data", Photogrammetric Engineering & Remote Sensing, vol. 56, no. 4, 1990, pp. 459-467.
- [8] Franklin S.E and Blodgett C.F., "An example of satellite multisensory data fusion", Computation Geoscience, vol.19, no. 4, 1993, pp. 577-583,
- [9] Wang Z, "A comparative analysis of image fusion methods", Geoscience and Remote Sensing, IEEE Transactions, vol.43, no.6, 2005, pp. 1391-1402.
- [10] Lillesand, T. M, and Kiefer, R. W., Remote Sensing and Image Interpretation, No. Ed. 5. John Wiley and Sons Ltd, 2004.
- [11] Mishra P, Singh D and Yamaguchi, Y., " Land cover classification of PALSAR images by knowledge based decision tree classifier and supervised classifiers based on SAR observables", Progress in Electromagnetics Research B, Vol. 30, 2011, pp. 47-70.
- [12] Ehsani, A. H., "Evaluation of Sequential Maximum a Posteriori (SMAP) Method for Land Cover Classification", Geomatics vol. 90 (National Conference & Exhibition), 2011.